Force Spectroscopy of Single-Chain Polysaccharides: Force-Induced Conformational Transition of Amylose Disappears under Environment of Micelle Solution

Chuanjun Liu, Zhiqiang Wang, and Xi Zhang*

Key Lab of Organic Optoelectronics and Molecular Engineering, Department of Chemistry, Tsinghua University, Beijing 100084, People's Republic of China, and Key Lab for Supramolecular Structure and Materials, College of Chemistry, Jilin University, Changchun 130012, People's Republic of China

Received January 10, 2006
Revised Manuscript Received March 16, 2006

Introduction. Single-molecule force spectroscopy (SMFS), an atomic force microscopy (AFM)-based technique, has been widely used to interpret the nanomechanical properties of both biomacromolecules and synthetic polymers.[1−17] Polysaccharides are important natural macromolecules in biological systems and play key roles in protein sorting, cell−cell communication, cell adhesion, and molecular recognition in the immune system.[18] Force spectroscopy on polysaccharides has aroused an increasing interest because AFM-based SMFS is a good tool for investigating the force-induced conformational transition, the dynamics, and supramolecular structures of polysaccharides at the molecular level.[6,7,19−24] Rief et al. first studied dextran, a linear α-(1,6)-linked polysaccharide, and observed a shoulder plateau at around 750 pN in the force profiles. Combined with molecular dynamics calculations, they attributed the plateau to the twist of the C5−C6 bond in the pyranose ring.[6] Marszalek et al. proved that it was the chair−boat conformational transition of the glucopyranose ring that governed the shoulder-like elongation by the cleavage of the ring structure.[7] By comparing α-(1,4)-linked and β-(1,4)-linked polysaccharides, Li et al. found that only α-(1,4)-linked glycan could yield a distinct elongation, and there were no such shoulders which appeared in β-(1,4)-linked polysaccharides.[19] The force-governed shoulder-like transition was thought to be the fingerprint property of α-(1,4)-linked glycan rings. Theoretical simulations on α-(1,4)-linked amylose and β-(1,4)-linked cellulose confirmed that only α-glucose has a fingerprint shoulder. To understand the force-induced conformational transition in a different viewpoint, the glycosidic bonds were regarded as atomic levers that drove the conformational changes of the pyranose ring.[20] By comparing the force spectroscopy on a series of carrageenans, we provided experimental evidence that the oxygen bridge could inhibit the transition.[21] Recently, Zhang et al. have reported that the force spectroscopy of amylose is solvent dependent. The plateau feature, which is characteristic of the force spectroscopy in water, disappears progressively in the media of lower dielectric constants.[24]

Although we have obtained more and more information about the force spectroscopy of polysaccharides, it remains unknown how a crowded environment influences the force-induced transition of polysaccharides. In crowded solutions the presence of many cosolutes often affects the properties of biopolymers, such as globular proteins. Important examples of crowded environments are those inside some cells, where protein stability or aggregation rates are affected by the presence of other coexisting molecules.[25−27] Since proteins, polysaccharides, and other biological macromolecules have evolved to function in crowded media, it is important to know how these molecules fold, interact, and move in such an environment. In this Communication, we investigate the change of force spectroscopy of single amylose chain in a crowded environment which is provided by micelles. Our research is aimed not only to understand the influence of the micelles on the force-induced conformational transition of polysaccharides but also to see whether the change of the force spectroscopy could indicate how crowded the environment is.

Experimental Section. a. Materials and Sample Preparation. Commercially available amylose (type III, from potato; Sigma-Aldrich Corp.), hexadecyltrimethylammonium bromide (CTAB), and sodium dodecyl sulfate (SDS) (Fluka, Corp.) were used without further purification in this study. Amylose was dissolved in water at a concentration of ∼0.01 mg/mL. In force experiments, quartz slides were used as substrate. The slides were treated with a hot "piranha" solution (7/3 volume ratio, 98% H_2SO_4/30% H_2O_2) and followed by extensive rinsing with water before the use. About 0.05 mL sample solution was deposited onto a cleaned quartz slide and incubated for about 30 min. Then the slide was rinsed with water to remove the loosely adsorbed molecules. After being dried by airflow, the slide was mounted onto the SMFS setup for force measurements.

b. Force Measurements. All force curves were measured by using the Molecular Force Probe 3D (MFP-3D; Asylum Research, Santa Barbara, CA). Silicon nitride cantilevers from Veeco (Santa Barbara, CA) were used. The spring constants of the cantilevers were calibrated by measuring their thermal fluctuation before force measurements,[28] and the measured values were 0.01−0.03 N/m. The velocity of the tip retraction during the force measurement was 2.0 μm/s, if not specified. The experimental details of SMFS have been described elsewhere.[29,30] In brief, amylose was immobilized onto the quartz substrate by physical adsorption. Prior to the measurements, a drop of liquid, acting as the buffer, was injected between the substrate and the cantilever holder, and then both the substrate and the cantilever were immersed in the buffer. By the movement of the piezotube, the AFM tip was brought in contact with the sample for ca. 2 s under a contact force of several nanonewtons, allowing some polymer chains to be physically adsorbed onto the tip, producing a connective bridge in between. During the separation of the tip and the sample, the polymer chain was stretched and the cantilever deflected. At the same time, a deflection−extension curve was recorded and then converted into a force−extension curve.

c. Interaction between Amylose and Surfactants. ^{1}H NMR and Fourier transform infrared (FT-IR) spectroscopy were employed to study the effect of the addition of surfactants on amylose chain. ^{1}H NMR spectra were recorded in D_2O solution on a JEOL JNM-ECA300 (300 MHz) spectrometer. FT-IR spectra of amylose and its mixture with surfactants were collected on a Bruker IFS 66V instrument equipped with a deuterated triglycine sulfate (DTGS) detector. The cell was fitted with CaF_2 windows and has a constant path length of 0.025 mm.

Results and Discussion. Before observing the force spectroscopy of single amylose in a crowded environment, we

* Corresponding author: e-mail xi@mail.tsinghua.edu.cn; Tel +86-10-62796283; Fax +86-10-62771149.

10.1021/ma060054e CCC: $33.50
Published on Web 04/19/2006

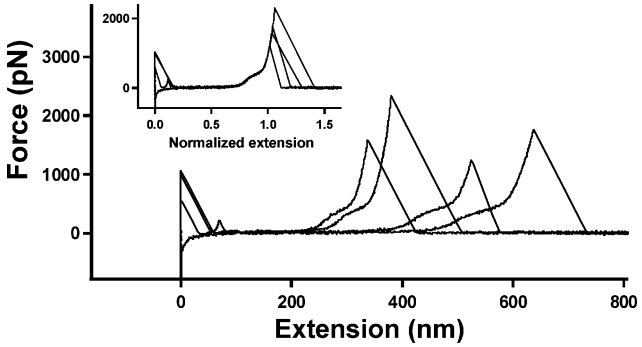

Figure 1. Several typical force−extension curves of amylose in water. The inset shows the superimposition of the normalized force−extension curves.

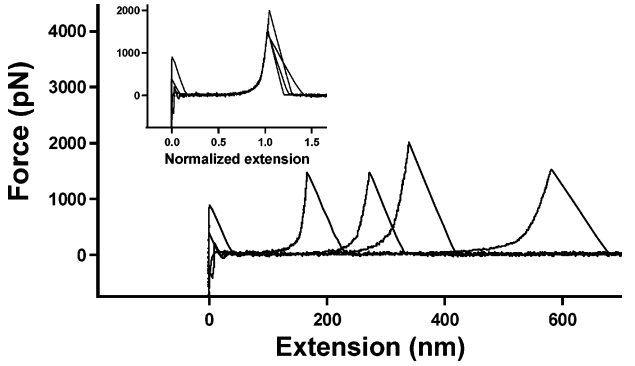

Figure 2. Several typical force−extension curves of amylose in 0.14 mol/L CTAB. The inset shows the superimposition of the normalized force−extension curves.

repeated the single-chain elongation of amylose under normal media of water. Several typical force−extension curves of amylose in water, obtained in different SMFS experiments with different cantilevers, are shown in Figure 1. There is a shoulder plateau about 280 pN high which appeared in each force−extension curve. The contour lengths of the polymer segment being stretched vary due to both the polydispersity of the polymer sample and the uncontrolled stretching point of the AFM tip. To compare the force−extension relationship of the polymer chains with different contour length, we normalized the curves by dividing the corresponding lengths measured under the same force of 1000 pN.[1,3] Despite different stretching lengths, the force−extension curves after the normalization can be well superimposed, as shown in the inset in Figure 1. The good superimposition of these curves clearly shows that the elastic properties of amylose chains scale linearly with the contour length, and all filaments show a transition at the same force. These results indicate that single-chain elongation is realized in these force experiments. As reported, the characteristic plateau in the force−extension curve of amylose is caused by the force-induced chair-to-boat transition of glucopyranose rings.[7,19]

To study the crowding effect on force spectroscopy of amylose, SMFS experiments were performed on single amylose chains in CTAB solution. It is well-known that CTAB can self-organize into micelles in water, when the concentration is above its critical micelle concentration (cmc).[31] Several typical force−extension curves of amylose obtained in the media of 0.14 mol/L CTAB are shown in Figure 2. The force rises monotonically with the increasing extension and then drops to zero rapidly until the rupture from the tip or the substrate. We also normalized these force−extension curves under the force value of 1000 pN. As indicated in the inset of Figure 2, the force

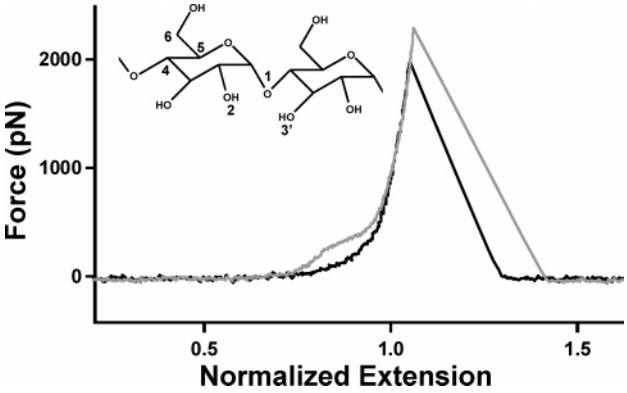

Figure 3. Comparison of normalized force−extension curves of amylose in water (gray trace) and in 0.14 mol/L CTAB (black trace). The inset shows a building block of amylose.

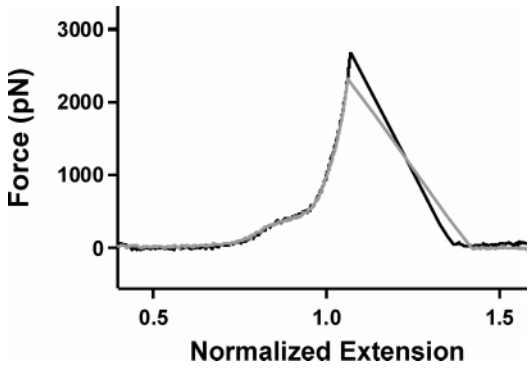

Figure 4. Comparison of normalized force−extension curves of amylose in water (gray trace) and in 0.014 mol/L CTAB (black trace).

curves can be well superimposed after being normalized, indicative of a single-chain elongation. When the normalized force−extension curves of amylose in water and in 0.14 mol/L CTAB were superimposed together, we observed a large deviation between them in the middle force region, as shown in Figure 3. It is interesting to find that the plateau feature, which is characteristic of the force spectroscopy of amylose in water, disappears in the media of 0.14 mol/L CTAB.

The two force−extension curves shown in Figure 3 are obtained in the media of pure water and CTAB solution, and the only difference is the environment of amylose chain during the force experiments. Therefore, it is reasonable to assume that the disappearance of plateau feature in the force−extension curves of amylose is related to the crowded environment in the micelle solution. To clarify the effect of solution environment on the force profiles of amylose, we performed a series of experiments by systematically changing the concentration of CTAB. When the concentration of CTAB is below 0.014 mol/L, the force−extension curve of amylose has shown a similar force profile as in water. As shown in Figure 4, the two normalized force−extension curves obtained in water and 0.014 mol/L CTAB are superimposed well in all force regions, suggesting that the existence of surfactant molecules does not influence the molecular elasticity of amylose if the concentration of CTAB is lower than 0.014 mol/L. The fact that only in a high concentration of CTAB the plateau feature in the force−extension curve disappeared indicates that the existence of large number of micelles affects the force-induced conformational transition of pyranose rings in amylose chain.

What is the mechanism behind the disappearance of the plateau in the force−extension curve of amylose chain in a high concentration of CTAB? The interaction between amylose and CTAB has been extensively investigated, suggesting that the

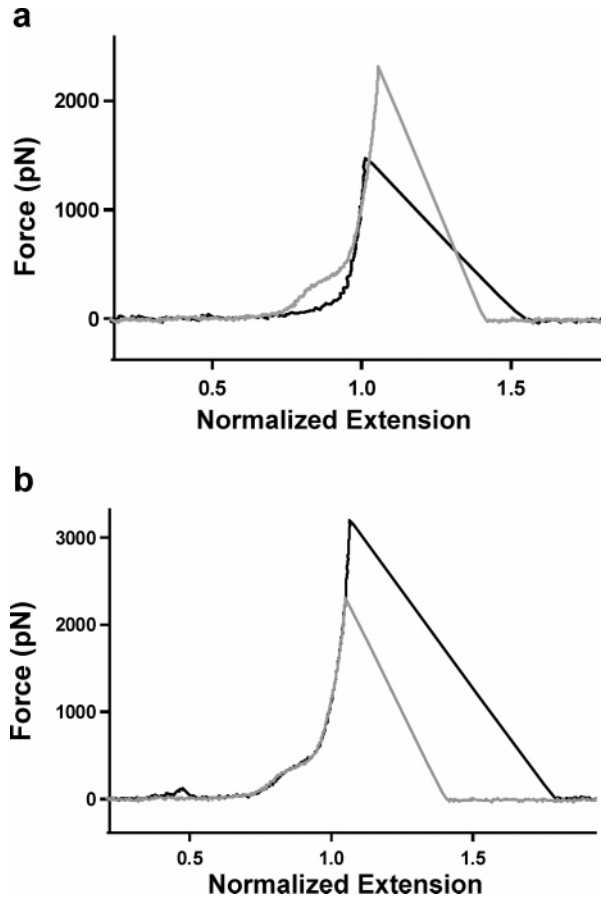

Figure 5. Force−extension curves of amylose obtained in SDS solution. (a) Comparison of normalized force−extension curves of amylose in water (gray trace) and in 0.18 mol/L SDS (black trace). (b) Comparison of normalized force−extension curves of amylose in water (gray trace) and in 0.018 mol/L SDS (black trace).

binding of CTAB to amylose is a cooperative process.[32−34] We speculate that the disappearance of plateau feature in the force−extension curve of amylose in high concentration of CTAB is related to the interaction between amylose and CTAB. Amylose can form strong inter-residue hydrogen bonding in a media of low dielectric constant or in solid state, and these hydrogen bonds are effectively eliminated in water because of the competition of glucose hydroxyls to form hydrogen bonds with water molecules.[24] Therefore, when the solution contains enough surfactant molecules, the interaction between CTAB and amylose chain might repel a large number of water molecules that should hydrate amylose. Because of the absence of water molecules around the amylose chain in a local environment, strong hydrogen bonds between adjacent rings are formed in amylose, which involve the interaction between O-2 and H-3′ atoms. The existence of these inter-residue hydrogen bonds results in the elimination of the plateau feature from the force−extension curves in high concentration of CTAB.[24]

To prove the above assumption, we employed ^{1}H NMR and FT-IR to study the influence of CTAB on amylose. The ^{1}H NMR signals of amylose (H-2,3,4,5) become more broader and less splitting upon the addition of CTAB (see Supporting Information, Figure S1). These changes indicate that the amylose chains are in a more hydrophobic environment upon addition of surfactants. Moreover, as indicated by FT-IR, the C−OH stretching vibration band of 1086 cm^{-1} undergoes a shift to longer wavelength (1081 cm^{-1}) upon the addition of CTAB, reflecting the change of different hydrogen bonding of amylose molecules before and after the addition of CTAB (see Supporting Information, Figure S2). On the basis of ^{1}H NMR and FT-IR, we may draw a conclusion that the addition of surfactants provide a more hydrophobic environment for amylose chain and then facilitate the formation of inter-residue hydrogen bonding.

If the above mechanism is reasonable, it is supposed to be true for crowded solution formed by other surfactants, for example, sodium dodecyl sulfate (SDS). To address this question, we performed similar single-chain elongation of amylose in the media of SDS solution. Figure 5a shows the comparison of the normalized force−extension curves of amylose in water and 0.18 mol/L SDS, from which we can find that the plateau feature in the force profiles of amylose also disappears. The force signals in SDS have shown similar characteristics as those in CTAB when the concentration is high. Whereas the concentration of SDS decreases to 0.018 mol/L, the force−extension curve of amylose has also shown a similar force profile as in water. As shown in Figure 5b, the two normalized force−extension curves obtained in water and 0.018 mol/L SDS superimpose well into all force regions, suggesting that the existence of surfactant molecules does not influence the molecular elasticity of amylose if the concentration of SDS is lower than 0.018 mol/L. These results further confirm that the existence of large number of micelles in the solution plays a key role in the force-induced conformational transition of amylose. Similarly, we employed ^{1}H NMR and FT-IR to study the interaction between amylose and SDS, and the results support the above conclusion from SMFS data (see Supporting Information, Figures S1 and S3).

Conclusions. We have studied the force spectroscopy of single-chain amylose in a media of crowded environment by using surfactant molecules as crowders. The plateau feature, which is characteristic of the force spectroscopy of amylose in water, disappears in the media of high concentration of CTAB or SDS. The SMFS experimental results indicate that the large number of micelles affects the force-induced conformational transition of pyranose rings of amylose chain and results in the change of force spectroscopy of amylose chain in high concentration of surfactants.

Acknowledgment. This study was supported by the Natural Science Foundation of China (20474035). We thank Prof. Liqiang Zheng for providing the surfactants and Prof. Yukihiro Ozaki for helpful discussions about FT-IR characterization.

Supporting Information Available: Details on ^{1}H NMR and FT-IR spectroscopy measurements.This material is available free of charge via the Internet at http://pubs.acs.org.

References and Notes

(1) Hugel, T.; Seitz, M. *Macromol. Rapid Commun.* **2001**, *22*, 989.
(2) Janshoff, A.; Neitzert, M.; Oberdörf, Y.; Fuchs, H. *Angew. Chem., Int. Ed.* **2000**, *39*, 3212.
(3) Zhang, W.; Zhang, X. *Prog. Polym. Sci.* **2003**, *28*, 1271.
(4) Evans, E. *Annu. Rev. Biophys. Biomol. Struct.* **2001**, *30*, 105.
(5) Butt, H. J.; Cappella, B.; Kappl, M. *Surf. Sci. Rep.* **2005**, *59*, 1.
(6) Rief, M.; Oesterhelt, F.; Heymann, B.; Gaub, H. *Science* **1997**, *275*, 1295.
(7) Marszalek, P.; Oberhauser, A.; Pang, Y.; Fernandez, J. *Nature (London)* **1998**, *396*, 661.
(8) Bemis, J. E.; Akhremitchev, B. B.; Walker, G. C. *Langmuir* **1999**, *15*, 2799.
(9) Schönherr, H.; Beulen, M.; Bügler, J.; Huskens, J.; van Veggel, F.; Vancso, G. J. *J. Am. Chem. Soc.* **2000**, *122*, 4963.
(10) Zou, S.; Schönherr, H.; Vancso, G. J. *Angew. Chem., Int. Ed.* **2005**, *44*, 956.
(11) Yamamoto, S.; Tsujii, Y.; Fukuda, T. *Macromolecules* **2000**, *33*, 5995.

(12) Conti, M.; Bustanji, Y.; Falini, G.; Ferruti, P.; Stefoni, S.; Samorì, B. *ChemPhysChem* **2001**, *2*, 610.
(13) Haupt, B.; Senden, T.; Sevick, E. *Langmuir* **2002**, *18*, 2174.
(14) Hugel, T.; Holland, B.; Cattani, A.; Moroder, L.; Seitz, M.; Gaub, H. *Science* **2002**, *296*, 1103.
(15) Zhang, D.; Ortiz, C. *Macromolecules* **2005**, *38*, 2535.
(16) Liu, C.; Cui, S.; Wang, Z.; Zhang, X. *J. Phys. Chem. B* **2005**, *109*, 14807.
(17) Long, J.; Xu, Z.; Masliyah, J. *Langmuir* **2006**, *22*, 1652.
(18) Dwek, R. A. *Chem. Rev.* **1996**, *96*, 683.
(19) Li, H.; Rief, M.; Oesterhelt, F.; Gaub, H.; Zhang, X.; Shen, J. *Chem. Phys. Lett.* **1999**, *305*, 197.
(20) Marszalek, P.; Pang, Y.; Li, H.; Yazal, J.; Oberhauser, A.; Fernandez, J. *Proc. Natl. Acad. Sci. U.S.A.* **1999**, *96*, 7894.
(21) Xu, Q.; Zhang, W.; Zhang, X. *Macromolecules* **2002**, *35*, 871.
(22) Zhang, L.; Wang, C.; Cui, S.; Wang, Z.; Zhang, X. *Nano Lett.* **2003**, *3*, 1119.
(23) Kawakami, M.; Byrne, K.; Khatri, B.; Mcleish, T.; Radford, S.; Smith, D. *Langmuir* **2004**, *20*, 9299.
(24) Zhang, Q.; Jaroniec, J.; Lee, G.; Marszalek, P. *Angew. Chem., Int. Ed.* **2005**, *44*, 2723.
(25) Minton, A. *J. Biol. Chem.* **2001**, *276*, 10577.
(26) Rivas, G.; Ferrone, F.; Herzfeld, J. *EMBO Rep.* **2004**, *5*, 23.
(27) Ping, G.; Yuan, J.; Sun, Z.; Wei, Y. *J. Mol. Recognit.* **2004**, *17*, 433.
(28) Butt, H. J.; Jaschke, M. *Nanotechnology* **1995**, *6*, 1.
(29) Li, H.; Liu, B.; Zhang, X.; Gao, C.; Shen, J.; Zou, G. *Langmuir* **1999**, *15*, 2120.
(30) Oesterhelt, F.; Rief, M.; Gaub, H. *New J. Phys.* **1999**, *1*, 6.1.
(31) Raman, N.; Anderson, M.; Brinker, C. *Chem. Mater.* **1996**, *8*, 1682.
(32) Yamamato, M.; Sano, T.; Harada, S.; Yasunaga, T. *Bull. Chem. Soc. Jpn.* **1983**, *56*, 2643.
(33) Bulpin, P. A.; Cutler, A. N.; Lips, A. *Macromolecules* **1987**, *20*, 44.
(34) Lundqvist, H.; Eliasson, A. C.; Olofsson, G. *Carbohydr. Polym.* **2002**, *49*, 43.

MA060054E